Research Report AS4103

Julián Proboste [1]

[1] Student of Astronomy - Computer Science, Universidad de Chile, julian.proboste@ug.uchile.com

Abstract

This work addresses the estimation of cosmological parameters from Cosmic Microwave Background (CMB) power spectra using simulation-based inference (SBI) methods. Unlike the traditional approach, which relies on Gaussian assumptions for the likelihood function, we employ modern inference techniques such as Sequential Neural Posterior Estimation (SNPE) and Neural Posterior Score Estimation (NPSE). Between 25,000 and 100,000 simulations of the power spectra C_ℓ^{TT}, C_ℓ^{EE}, C_ℓ^{BB}, and C_ℓ^{TE} were generated using the CAMB code, considering only scalar modes. The results show that NPSE provides wider but less biased posterior distributions compared to SNPE, thus improving the robustness of the inference. Furthermore, we analyze the well-known degeneracy between the optical depth to reionization τ and the primordial amplitude A_s, showing that the inclusion of low-ℓ polarization data is crucial to properly constrain these parameters. Overall, this study demonstrates the potential of SBI methods as a flexible and efficient alternative to traditional Bayesian approaches in cosmology.

1 Introduction

1.1 Cosmological Context

The discovery of the Cosmic Microwave Background (CMB) by Arno Penzias and Robert Wilson [1] in 1965 confirmed the existence of isotropic microwave radiation permeating the universe. Subsequent experiments showed that this radiation follows a blackbody spectrum with a temperature of $T = 2.7255\,\mathrm{K}$ [2]. The energy density of the CMB is low, with approximately 411 photons per cubic centimeter, and its characteristic wavelength ($\sim 2\,\mathrm{mm}$) places it in the microwave region of the electromagnetic spectrum [2].

The existence of the CMB constituted key evidence in favor of the Big Bang model over the Steady State model. In an expanding universe that was initially hot and dense, matter was ionized, making the universe opaque. As the universe expanded and cooled, electrons and protons combined to form neutral atoms, allowing photons to decouple from matter. This radiation, which originally had a temperature of $\sim 2970\,\mathrm{K}$, has cooled to the current $2.7255\,\mathrm{K}$ due to cosmic expansion [2].

With the arrival of the *WMAP* and *Planck* probes, high-precision measurements of CMB anisotropies were achieved, which are fundamental for understanding the primordial inhomogeneities that gave rise to the large-scale structure of the universe. Combining these results with independent observations, such as type Ia supernovae and galaxy distribution, has allowed for refined estimates of cosmological parameters, consolidating the ΛCDM model as the standard framework of modern cosmology.

1.2 Traditional Inference

In modern cosmology, CMB analysis follows a well-established methodology, which now faces new challenges due to the volume and complexity of current data. The starting point is the temperature and polarization maps obtained by missions such as Planck [3] and, in the near future, the Simons Observatory [4]. These maps contain primordial information about both cosmological parameters and the initial conditions of the universe.

Traditional analysis takes these maps and extracts the power spectra C_ℓ^{TT}, C_ℓ^{EE}, C_ℓ^{TE}, and C_ℓ^{BB}, which quantify angular correlations at different scales ($\ell \sim 180^\circ/\theta$). This compression preserves Gaussian information and reduces data dimensionality. Mathematically, the power spectra correspond to the coefficients in the Legendre polynomial expansion of the two-point correlation function:

$$C(\theta) = \sum_{\ell=0}^{\infty} \frac{2\ell+1}{4\pi} C_\ell P_\ell(\cos\theta) \tag{1}$$

where the two-point correlation function $C(\theta)$ is defined as:

$$C(\theta) = \langle T(\hat{n}_1) T(\hat{n}_2) \rangle \tag{2}$$

with $T(\hat{n})$ being the temperature field in the unit direction $\hat{n}$. The inference of cosmological parameters is carried out through likelihood functions, usually Gaussian, that compare observed spectra with theoretical predictions. Bayesian inference combines these likelihoods with prior distributions incorporating theoretical knowledge and independent constraints. In practice, exploration of the parameter space is typically performed using Markov Chain Monte Carlo (MCMC) methods, which sample the posterior distribution in high-dimensional spaces.

This approach has allowed precise determination of the ΛCDM model parameters but requires assuming a likelihood function that is not always exact. Moreover, the Gaussian likelihood assumption may be too restrictive. In the following section, an alternative simulation-based approach is presented, which allows inference in situations where the likelihood is intractable or unknown.

1.3 Simulation-Based Inference

The traditional approach presents two fundamental limitations: the loss of non-Gaussian information during compression to power spectra, and the dependence on Gaussian assumptions in the likelihood. Both problems are closely related, since attempting inference with non-Gaussian summary statistics while assuming a Gaussian likelihood can lead to biased results. Simulation-based inference (SBI) aims to perform statistical inference in situations where the likelihood function is intractable or unknown.

Hybrid methods such as ABC (*Approximate Bayesian Computation*) address this problem by directly comparing simulated data with ob-

served data using a distance metric. In this approach, multiple simulations are generated from different parameter values θ and those for which the simulated data x sufficiently resemble the observed data, according to a tolerance threshold, are retained. This method strongly depends on the choice of summary statistics and may require a very large number of simulations to obtain a reasonable approximation of the posterior distribution.

More recently, modern machine learning-based techniques such as SNPE (*Sequential Neural Posterior Estimation*) [5] or NPSE (*Neural Posterior Score Estimation*) [6] [7] have revolutionized this approach. Instead of directly comparing data, these methods reformulate the problem as one of density estimation: the joint distribution of simulated pairs (θ, x) is modeled, allowing approximation of the posterior distribution $p(\theta|x)$. Tools such as deep neural networks and normalizing flows enable training expressive models that learn directly the relationship between data and parameters from synthetic samples, avoiding the explicit computation of the likelihood and making inference much more efficient.

1.4 Project Objective

The main objective of this project is the implementation of simulation-based inference techniques to estimate cosmological parameters from angular power spectra of the CMB. In the methodology section, the problem is introduced and the proposed methodology is described, while the results section presents the outcomes obtained using the proposed approach.

2 Methodology

2.1 Cosmological Parameters

We considered the parameters of the ΛCDM model introduced in the Markov chains by the *Planck Collaboration 2018* [3], namely the reduced density contrast of cold dark matter ω_c and baryons ω_b, the angular scale of the sound horizon at recombination θ_{MC}, the amplitude of the primordial spectrum A_s, the spectral index n_s, and the optical depth to reionization τ. Initially, only the first five cosmological parameters were used, leaving out the optical depth τ. This was due to its well-known temperature degeneracy with the parameter A_s [8].

2.2 Simulations

Since a large number of power spectra need to be simulated by varying the cosmological parameters, it is necessary to adopt a probability distribution from which to initially draw these parameters, known as the prior. In this project, a flat prior was used within a range of ±10 sigmas around the fiducial values reported by the *Planck Collaboration 2018* [3].

Between 25,000 and 100,000 random samples were drawn from the prior, and for each cosmology a power spectrum of each type (C_ℓ^{TT}, C_ℓ^{EE}, C_ℓ^{BB}, C_ℓ^{TE}) was simulated in the multipole range $0 \leq \ell \leq 2500$. The simulations included only scalar modes (tensor-to-scalar ratio $r = 0$) and accounted for lensing effects. These simulations were carried out using the CAMB framework in Python [9]. Figure 1 shows three examples for each simulated power spectrum.

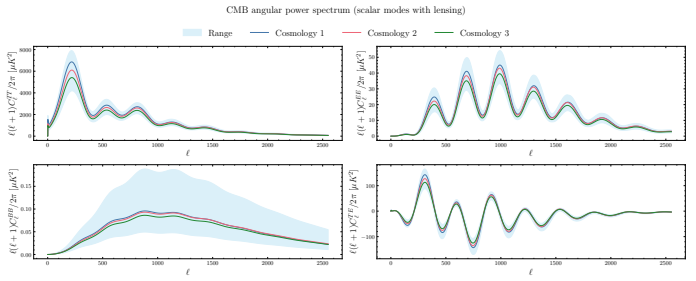

Figure 1: Example of three simulations of the power spectra C_ℓ^{TT}, C_ℓ^{EE}, C_ℓ^{BB}, C_ℓ^{TE}, respectively. Each simulation was generated from a random sample of the prior.

2.3 Inference Models

To estimate the posterior distribution of the cosmological parameters, different inference models were used. In particular, *Sequential Neural Posterior Estimation* [5] (SNPE) and *Neural Posterior Score Estimation* (NPSE) [6] [7] were employed, implemented in the *SBI* Python framework [10]. Both NPSE and SNPE are Bayesian inference methods for simulation-based models, but they differ in their representation of the posterior and their training mechanisms. NPSE uses conditional diffusion models and *score matching* to estimate density gradients, thereby avoiding the use of normalizable models [6], while SNPE employs *normalizing flows* to directly model the posterior and requires importance-weighting corrections [5]. In the specific case of this project, NPSE showed better adaptation to the data, producing wider but less biased posteriors than SNPE, as shown in Figure 2.

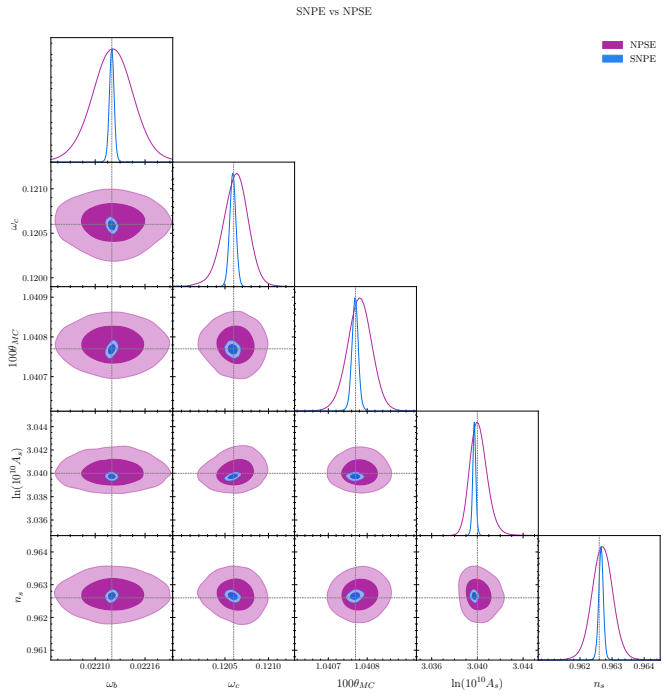

Figure 2: PPC diagnostic of the results obtained with the inference models SNPE and NPSE. Both models were trained with the same 100,000 simulations of the C_ℓ^{TT} power spectrum. The dashed line indicates the true value of the parameters. The NPSE model yields wider but less biased distributions compared to SNPE.

2.4 Posterior Predictive Check (PPC)

The result of training the selected inference model is known as a density estimator, which is capable of generating random samples from the trained posterior distribution given an observation. To analyze and evaluate the quality of the model, the *Posterior Predictive Check* (PPC) [10] method was used. This consists of selecting a true value for the cosmological parameters and simulating an observed power spectrum, and then sampling the previously trained posterior distribution from this observation. In this way, the posterior distribution obtained by the inference model can be compared with the true parameter value, typically represented by a dashed line, as shown in Figure 2.

3 Results

3.1 Inference without reionization parameter

Since the parameter τ has a known physical degeneracy with the parameter A_s [8], the set of six parameters was temporarily reduced to five, with τ later added back. The results of training NPSE inference models with the power spectra C_ℓ^{TT}, C_ℓ^{EE}, C_ℓ^{BB}, and C_ℓ^{TE} in the range $0 \leq \ell \leq 2500$ are shown in Figure 3.

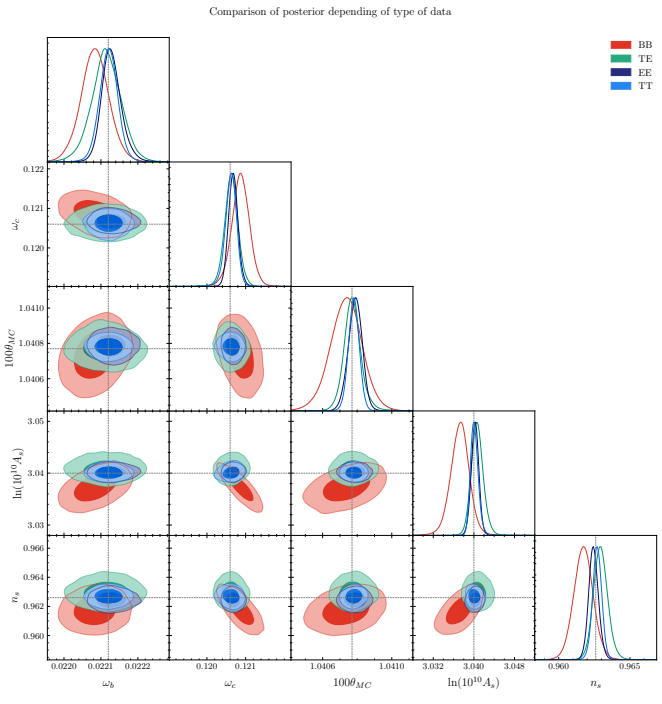

Figure 3: NPSE inference models trained with 100,000 simulations of the power spectra C_ℓ^{TT}, C_ℓ^{EE}, C_ℓ^{BB}, and C_ℓ^{TE}. Each color represents a model trained with a different power spectrum. The dashed line shows the true value of the parameters.

The results show how the choice of dataset (C_ℓ^{TT}, C_ℓ^{EE}, C_ℓ^{BB}, C_ℓ^{TE}) affects the posterior distributions of the selected cosmological parameters. The variation in ω_b, ω_c, n_s, $\ln(10^{10}A_s)$, and $100\theta_{MC}$ is small but non-negligible, reflecting the sensitivity of each parameter to the type of information included. In particular, the temperature and E-mode spectra (TT, EE, TE) introduce slight tensions compared to the B-mode spectrum (BB), highlighting the lack of information contained in the B-mode spectra computed only from scalar perturbations, without including primordial B-modes. Figure 9 shows the comparison between the power spectra corresponding to the true parameters and those corresponding to a random sample from the posterior distribution obtained by training an NPSE inference model with 100,000 simulations of the C_ℓ^{TT} power spectrum.

3.2 Inference with reionization parameter

When the parameter τ is included, the full set of six cosmological parameters is recovered. Figure 4 shows the results obtained by training the NPSE inference model with 100,000 simulations including τ. This parameter introduces a clear degeneracy with A_s, which results in a broadening and a slight bias in the posterior distribution of both parameters compared to the case without τ, as well as an elongation of their joint distribution.

Moreover, the inclusion of τ produces slight variations in the posterior distributions of n_s and ω_c, although these remain within statistical dispersion. The temperature (TT) and polarization (EE, TE) spectra, particularly at large scales, provide the strongest sensitivity to the value of τ, while the TT modes at high multipoles are unable to break the degeneracy. Consequently, this confirms the necessity of incorporating information from the first 30 multipoles of the polarization spectra (lowEE, lowTE) to improve the precision in the estimation of τ and, therefore, of A_s.

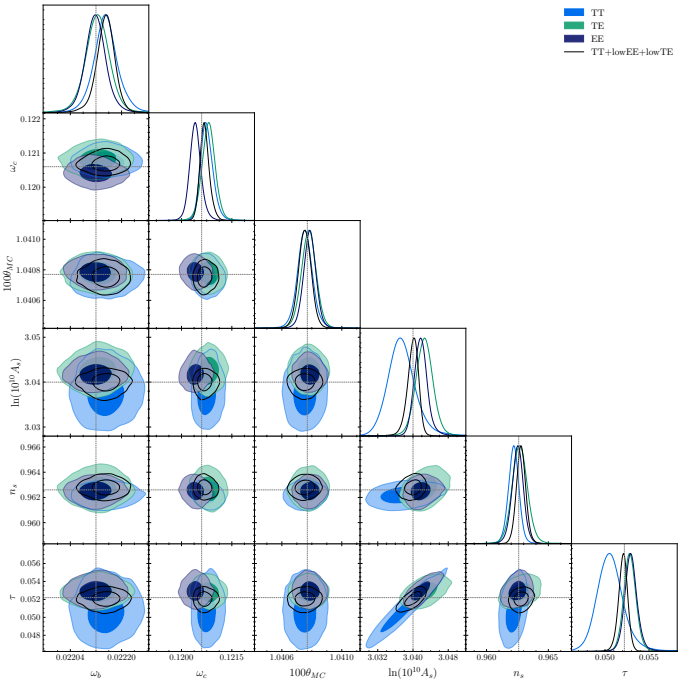

Figure 4: Results of NPSE inference considering the six standard cosmological parameters, including τ. The degeneracy between τ and $\ln(10^{10}A_s)$ is evident, producing a broadening of their posterior distributions. The different datasets (TT, TE, EE, and TT+lowEE+lowTE) highlight the importance of including low-multipole information to constrain the value of τ.

3.3 Adding Noise

To approximate more realistic observational conditions, noise is introduced into the simulations of the power spectra C_ℓ^{TT}. We mainly consider two sources: the instrumental noise of the experiment and the partial sky coverage, which adds additional cosmic variance. First, instrumental noise is incorporated into the theoretical spectra using a model based on the angular resolution of the instrument (θ_{fwhm}) and the pixel sensitivity (σ_T) [11]. The instrumental noise term N_ℓ^{TT}, which is added to the theoretical power spectrum C_ℓ, is defined as:

$$N_\ell^{\text{TT}} = (\theta_{\text{fwhm}} \cdot \sigma_T)^2 \exp\left[\ell(\ell+1)\frac{\theta_{\text{fwhm}}^2}{8\ln 2}\right], \tag{3}$$

where θ_{fwhm} is expressed in radians. This expression models the sky smoothing due to the finite resolution of the instrument.

Subsequently, the observation of a partial sky is simulated, considering that only a fraction $f_{\text{sky}} < 1$ of the full sky is measured. As a result, the observable estimator of C_ℓ, denoted $\hat{C}_\ell$, becomes a random variable whose dispersion depends on f_{sky}. For low multipoles ($\ell < \ell_{\text{transition}}$), this variance is modeled through a scaled chi-squared distribution:

$$\hat{C}_\ell = \frac{1}{\nu_\ell}\sum_{i=1}^{\nu_\ell} X_i^2, \quad X_i \sim \mathcal{N}(0, \sqrt{C_\ell}), \tag{4}$$

where $\nu_\ell = \text{round}(f_{\text{sky}} \cdot (2\ell+1))$ represents the effective number of degrees of freedom. This formulation correctly captures the statistical dispersion of the estimator when the number of available modes is limited. For high multipoles ($\ell \geq \ell_{\text{transition}}$), it is assumed that the estimator can be approximated by a normal distribution centered on C_ℓ with variance:

$$\hat{C}_\ell \sim \mathcal{N}\left(C_\ell, \frac{2C_\ell^2}{f_{\text{sky}}(2\ell+1)}\right). \tag{5}$$

This Gaussian approximation is valid thanks to the central limit theorem, since in this regime the number of available modes is sufficiently large.

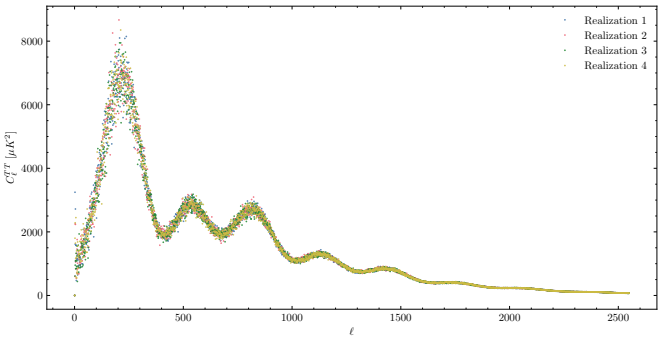

Figure 5: Multiple realizations of a power spectrum for the same combination of cosmological parameters, including instrumental noise and the effect of partial sky coverage. Each color represents a different realization.

To capture the randomness introduced by noise in the power spectra, multiple realizations of each combination of cosmological parameters were generated in the training set [12]. Each cosmology was simulated several times, applying instrumental noise and the variance associated with partial sky coverage, so that the model can learn the natural dispersion of the observables due to these sources of uncertainty. This approach allows the inference model not only to learn the average values of the spectra, but also to internalize the statistical variability caused by noise. In this way, the posterior predictions more realistically reflect the uncertainty expected in real observational data.

Figure 5 shows an example of multiple realizations of the power spectrum for the same cosmology, where each colored line represents a different realization. It can be observed how noise produces significant variations in the spectrum, especially at scales where instrumental noise and partial sky coverage have the greatest effect.

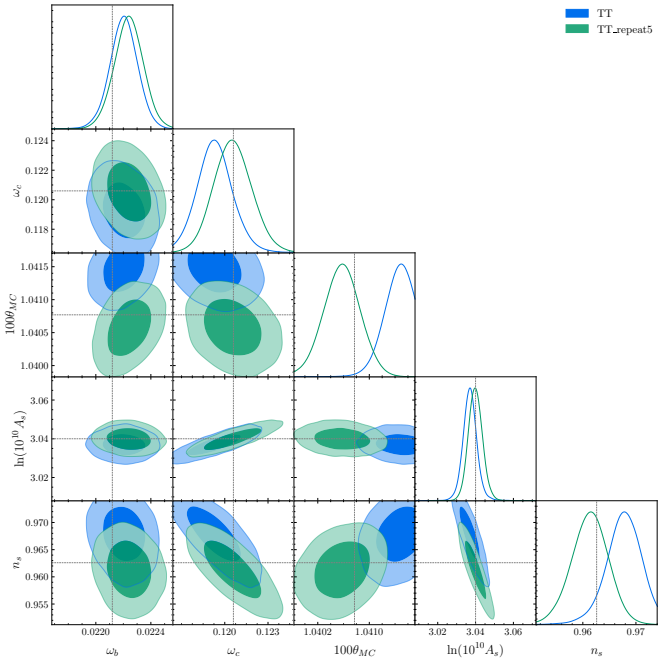

Figure 6: Inference of cosmological parameters from the TT power spectrum. The model training without additional realizations (`TT`) is compared to the case with five noisy realizations per cosmology (`TT repeat5`). These NPSE models were trained with 100,000 base cosmologies.

Figure 6 presents the posterior distributions of cosmological parameters obtained under two training schemes. In the case without additional realizations (blue plot), the distributions appear narrower, reflecting an underestimation of the true uncertainty associated with the data. In contrast, when five noisy realizations per cosmology are included in the training (green plot), the posteriors are more consistently centered and capture more faithfully the dispersion induced by instrumental noise.

Although the scheme with realizations still shows residual artificial degeneracies and biases, the results are significantly improved compared to the scheme without realizations. Most parameters exhibit intervals that are closer to the expected statistical variability, indicating that the model, when exposed to multiple realizations, better internalizes the stochastic nature of the data and avoids an overconfident characterization of the posteriors.

4 Conclusion

Lorem ipsum dolor sit amet, consectetur adipiscing elit, sed do eiusmod tempor incididunt ut labore et dolore magna aliqua. Ut enim ad minim veniam, quis nostrud exercitation ullamco laboris nisi ut aliquip ex ea commodo consequat. Duis aute irure dolor in reprehenderit in voluptate velit esse cillum dolore eu fugiat nulla pariatur. Excepteur sint occaecat cupidatat non proident, sunt in culpa qui officia deserunt mollit anim id est laborum

5 Appendix

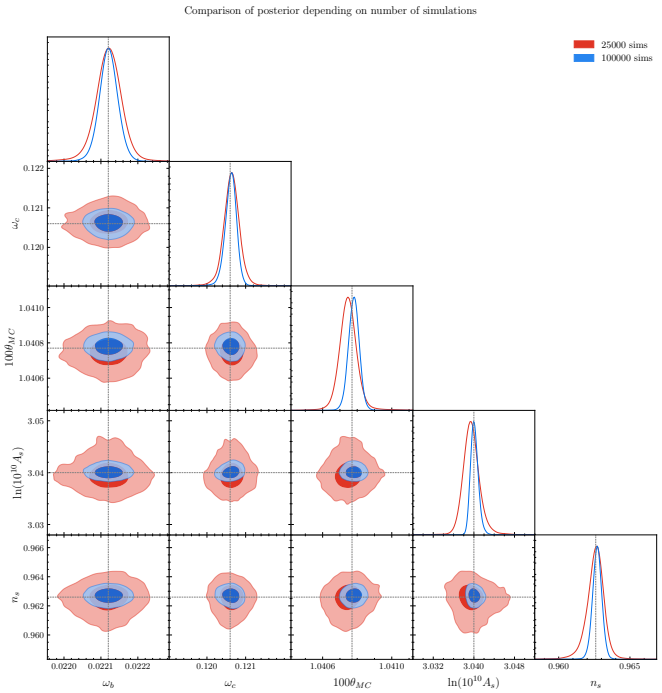

Figure 7: PPC diagnostic of the inference performed with 25,000 and 100,000 training simulations of the C_ℓ^{TT} power spectrum. Both models were trained with the NPSE architecture. The dashed line shows the true value of the parameters. The model trained with 100,000 simulations exhibits better convergence than the one trained with 25,000 simulations, with a more concentrated distribution and smoother boundaries.

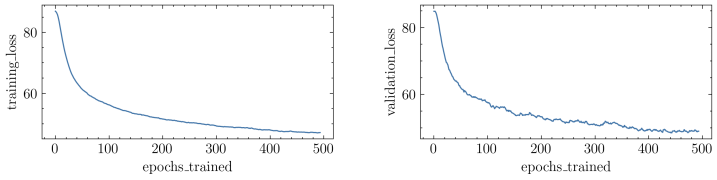

Figure 8: Evolution of the loss function on training and validation sets across 500 epochs. The NPSE model was trained with 100,000 simulations of the C_ℓ^{TT} spectrum.

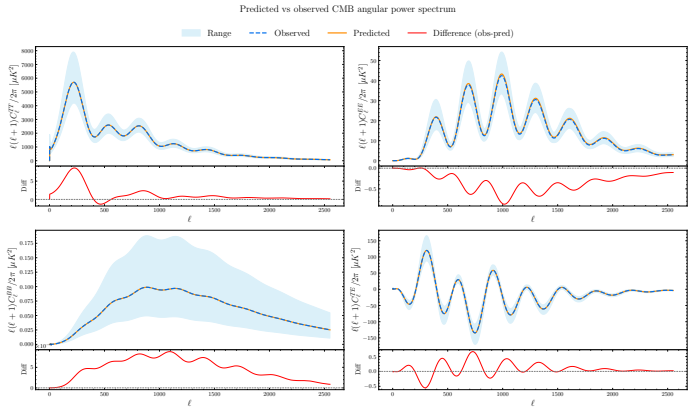

Figure 9: Comparison of the power spectra C_ℓ^{TT}, C_ℓ^{EE}, C_ℓ^{BB}, and C_ℓ^{TE} simulated with the true parameter values and the power spectra obtained from a random posterior sample derived from training an NPSE inference model with 100,000 simulations of the C_ℓ^{TT} power spectrum. The lower panel of each subplot shows the difference between the observed and predicted power spectra.

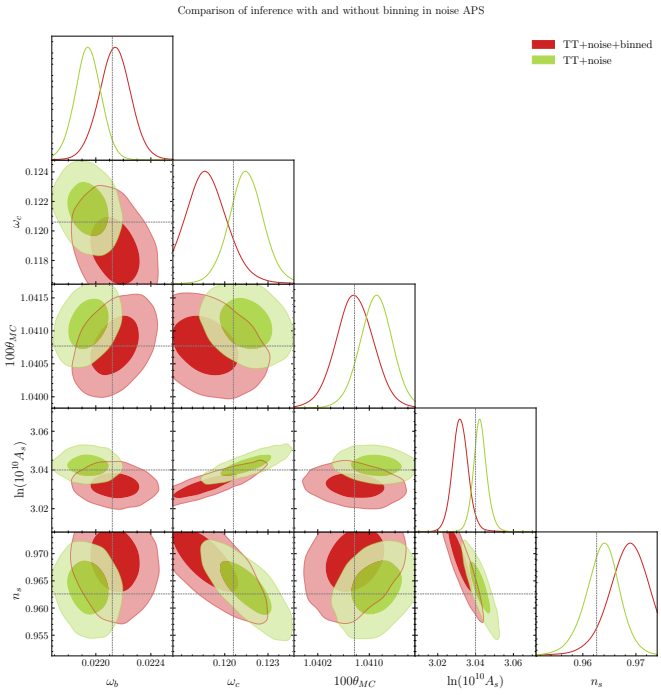

Figure 10: Comparison of cosmological inference from the TT power spectrum, considering two training schemes: with unbinned noise (`TT+noise`) and with noise averaged over 500 bins (`TT+noise+binned`). These NPSE models were trained with 100,000 base cosmologies

References

[1] Penzias, A. A. y Wilson, R. W., "A measurement of excess antenna temperature at 4080 mc/s", The Astrophysical Journal, 1965, doi:10.1086/148307.

[2] Ryden, B., Introduction to Cosmology. Cambridge University Press, 2 ed., 2017.

[3] Collaboration, P., "Planck 2018 results. VI. cosmological parameters", arXiv preprint arXiv:1807.06209, Jun 2018.

[4] Collaboration, S. O., "The simons observatory: Science goals and forecasts", arXiv preprint arXiv:1808.07445, Mar 2019.

[5] Greenberg, D. S., Nonnenmacher, M., y Macke, J. H., "Automatic posterior transformation for likelihood-free inference", arXiv preprint arXiv:1905.07488, May 2019.

[6] Sharrock, L., Simons, J., Liu, S., y Beaumont, M., "Sequential neural score estimation: Likelihood-free inference with conditional score based diffusion models", arXiv preprint arXiv:2210.04872, Jun 2024.

[7] Geffner, T., Papamakarios, G., y Mnih, A., "Compositional score modeling for simulation-based inference", arXiv preprint arXiv:2209.14249, Jul 2023.

[8] Hu, W. y White, M., "A cmb polarization primer", 1997, doi:10.1016/S1384-1076(97)00022-5.

[9] Lewis, A., "Camb: Code for anisotropies in the microwave background", 2023. Accessed: 2025-07-11.

[10] Tejero-Cantero, A., Boelts, J., Deistler, M., Lueckmann, J.-M., Durkan, C., Goncalves, P. J., Greenberg, D., y Macke, J. H., "sbi: A toolkit for simulation-based inference", 2020, doi:10.21105/joss.02505.

[11] Cole, A., Miller, B. K., Witte, S. J., Cai, M. X., Grootes, M. W., Nattino, F., y Weniger, C., "Fast and credible likelihood-free cosmology with truncated marginal neural ratio estimation", arXiv preprint arXiv:2111.08030, 2021, https://doi.org/10.48550/arXiv.2111.08030. Submitted on 15 Nov 2021 (v1), last revised 8 Nov 2022 (v2).

[12] Novaes, C. P., Thiele, L., Armijo, J., Cheng, S., Cowell, J. A., Marques, G. A., Ferreira, E. G. M., Shirasaki, M., Osato, K., y Liu, J., "Cosmology from hsc y1 weak lensing with combined higher-order statistics and simulation-based inference", arXiv preprint arXiv:2409.01301, 2024, https://doi.org/10.48550/arXiv.2409.01301. Submitted on 2 Sep 2024.